Heat transfer in protein–water interfaces

Anders Lervik,[ab] Fernando Bresme,*[ac] Signe Kjelstrup,[bc] Dick Bedeaux[bc] and J. Miguel Rubi[cd]

Received 8th September 2009, Accepted 3rd December 2009
First published as an Advance Article on the web 11th January 2010
DOI: 10.1039/b918607g

We investigate using transient non-equilibrum molecular dynamics simulation the temperature relaxation process of three structurally different proteins in water, namely; myoglobin, green fluorescence protein (GFP) and two conformations of the Ca^{2+}-ATPase protein. By modeling the temperature relaxation process using the solution of the heat diffusion equation we compute the thermal conductivity and thermal diffusivity of the proteins, as well as the thermal conductance of the protein–water interface. Our results indicate that the temperature relaxation of the protein can be described using a macroscopic approach. The protein–water interface has a thermal conductance of the order of 100–270 MW K^{-1} m^{-2}, characteristic of water–hydrophilic interfaces. The thermal conductivity of the proteins is of the order of 0.1–0.2 W K^{-1} m^{-1} as compared with $\approx$0.6 W K^{-1} m^{-1} for water, suggesting that these proteins can develop temperature gradients within the biomolecular structures that are larger than those of aqueous solutions. We find that the thermal diffusivity of the transmembrane protein, Ca^{2+}-ATPase is about three times larger than that of myoglobin or GFP. Our simulation shows that the Kapitza length of these structurally different proteins is of the order of 1 nm, showing that the protein–water interface should play a major role in defining the thermal relaxation of biomolecules.

Introduction

Biological molecules have developed mechanisms and structures that enable the efficient and rapid dissipation of excess energy through the biomolecule structure itself and through the biomolecule–solution interface. Finding the microscopic mechanism controlling energy transport in biomolecules represents a considerable challenge, which could provide a basis to understand complex biological processes. It is accepted that the timescale associated with the energy relaxation throughout the molecule can influence the kinetics of biomolecule reactions.[1] Similarly the pathways followed by the energy during the relaxation process can provide important clues to understand allostery.[2] In order to rationalize these processes, some questions must be addressed, *e.g.*, how perturbations occurring at a specific spot in the biomolecule, namely, binding of small molecules at receptor sites, may impart a conformational change at a distant spot, lying several nanometres away.[3] This question is very relevant to understanding how biomolecular motors, such as Ca^{2+}-ATPase, work. Ca^{2+}-ATPase requires the hydrolysis of ATP to enable Ca^{2+} transport. In this instance, the spot where the hydrolysis takes place and the binding site for the Ca^{2+} ions, are separated by about 4 nm.[4] It is expected that the energy transfer between these sites may involve the concerted motion of hundreds to thousands of atoms. Studies on different proteins suggest that there might be a set of residues that configure the energy pathway. This energy pathway would be an inherent property of the protein's tertiary structure, and could provide the microscopic basis for signal transduction.[5]

Chemical and photochemical reactions occurring at specific spots in biomolecules can result in large increases in temperature in very small volumes. Transient photon experiments, where photon absorption is converted to vibrational energy, show that the temperature rise resulting from this process can be very significant, between 500 and 1000 K.[6,7] Recent work on the Ca^{2+}-ATPase embedded in the sarcoplasmic reticulum has suggested that this enzyme can—under working conditions—release significant amounts of heat. Using micro-thermometers it was found that thermal gradients of the order of 10^5 K m^{-1} can develop between regions separated by tens of micrometres.[8] These temperature gradients could lead to interesting coupling effects, such as water polarization, which has been predicted very recently.[9]

The quantification of thermal transport in biomolecules in terms of a few bio-material properties, *e.g.* the thermal diffusivity, has been discussed recently.[10] Experimental and theoretical studies have provided important insights on the vibrational energy relaxation and energy pathways in proteins. Using picosecond anti-Stokes resonance Raman spectroscopy it has been possible to monitor the cooling dynamics of myoglobin.[11] It is expected that in addition to the energy relaxation occurring inside the protein, vibrational energy can also flow through the protein–solvent interface. Experiments of peptide chains in an

[a] *Department of Chemistry, Imperial College London, London, UK SW7 2AZ. E-mail: f.bresme@imperial.ac.uk*
[b] *Department of Chemistry, Norwegian University of Science and Technology, NO-7491, Trondheim, Norway*
[c] *Center for Advanced Study at the Norwegian Academy of Sciences and Letters, NO-0271, Oslo Norway*
[d] *Departamento de Física Fonamental, Facultad de Física, Universidad de Barcelona, E-08028, Spain. E-mail: fbresme@imperial.ac.uk*

organic solvent indicate that a significant amount of dissipation can occur through the molecule–solvent interface.[7] The time scale associated with such processes has also been estimated, being of the order of tens of picoseconds in myoglobin.[12] This time scale is not far from the one associated to the relaxation through the biomolecular structure, indicating that a vibrational coupling between biomolecular and solvent degrees of freedom may take place.[13]

Computer simulation techniques are being used to investigate the transport properties as well as vibrational energy pathways of proteins.[6,7,10,12,14–28] These studies have reported vibrational energy relaxation times between one to several tens of picoseconds. The first simulation study of vibrational energy relaxation of heme proteins was reported in ref. 6. These simulations relied on the injection of vibrational energy by an amount equivalent to the energy associated to photon absorption. Subsequent methodologies have exploited the scaling of the energy diffusion coefficient with the vibrational mode frequency of a protein,[10] or have modelled the heat transfer process as a boundary thermal transport problem.[14–16] These simulation methods offer the possibility of estimating transport coefficients, particularly the thermal diffusivity and the thermal conductivity. In this way it has been shown that the thermal conductivity of several proteins, myoglobin, ribonuclease T1, and green fluorescent protein GFP, is smaller than that of water, about 200–300 mW K^{-1} m^{-1}.[10,16,23] This value is similar to the thermal conductivity of hydrocarbon liquids[29] and hydrocarbon nanodroplets.[30] In addition to quantifying transport coefficients, computer simulations provide a unique approach to interpret the vibrational relaxation process in terms of intermolecular interactions. As a matter of fact, it has been shown that the electrostatic interaction of the isopropionate side chains of myoglobin with the surrounding solvent, provides a mechanism for kinetic energy dissipation.[19,20]

Previous experimental and simulation studies indicate that the solvent surrounding a protein can enhance the dissipation of vibrational energy associated with high temperature regions inside the protein. It is expected that the thermal conductance of the protein–water interface may play an important role in determining the efficiency of this relaxation process. We have recently shown[30] that the interface curvature strongly affects the magnitude of the interfacial thermal conductance. This effect is particularly important at the nanometre scale characteristic of nanoparticles, and is hence expected to be relevant also in biological nanoparticles (proteins).

In this article we have used transient non-equilibrium molecular dynamics to compute the thermal conductance of the protein–water interface for three structurally different proteins, namely: myoglobin, the green fluorescence protein and two conformations of the Ca^{2+}-ATPase. The latter is an example of an important family of molecular motors. Using the non-equilibrium thermodynamics theory, non-linear flux-force relations for conversion of chemical to osmotic and thermal energy have been derived recently.[31–33] It has been possible to obtain an expression for the measurable heat flux out of the ATPase and the vesicle it was embedded in. In order to do this it was assumed that the temperature of the ATPase was the same as that of the vesicle interior. This assumption remains unsupported. Hence, in order to further establish the validity of these assumptions it is necessary to investigate the thermal properties of proteins, and study their dissipation of energy.

The paper is structured as follows. Firstly we discuss the methodology employed in this work; the transient non-equilibrium molecular dynamics simulations and the equations employed to analyze the temperature relaxation in the proteins. The discussion of our results including the heat capacity of the proteins as well as the thermal conductivity and thermal conductance follows. We finish the paper with the main conclusions obtained in this work.

Methodology

Transient non-equilibrium molecular dynamics

The interfacial conductance can be computed using stationary non-equilibrium molecular dynamics (NEMD) simulations, whereby a temperature gradient is imposed in a direction perpendicular to the interface plane.[34–38] This methodology has been used to compute the interfacial conductance, or the inverse of this quantity—the interfacial resistivity—of alkane–water and alkane–vapor interfaces.[37,38] In addition to stationary methods, non stationary NEMD or transient NEMD has been employed to investigate biomolecules.[14,16] This method explicitly models the protein–water interface by immersing the protein in a solvent. The protein and the solvent are set initially at different temperatures, and the temperature relaxation is monitored over time. The temperature relaxation curve is fitted to a solution of the heat diffusion equation, which can be used to estimate the interface thermal conductance as well as the thermal conductivity and diffusivity. Many computational studies assume a first order process in which the temperature relaxation is modeled as a simple exponential decay. We have considered recently an analysis that goes beyond a pure first order process, and that incorporates as a variable the thermal conductivity and the temperature discontinuity arising at the protein–water interface, due to the acoustic mismatch of the protein and the solvent.[30] This is the approach we use in this work. For completeness it is discussed below.

The temperature relaxation can be modeled using the heat diffusion equation (in spherical coordinates),

$$\frac{1}{r^2}\frac{\partial}{\partial r}\left(\kappa r^2 \frac{\partial T(r,t)}{\partial r}\right) = \rho c_p \frac{\partial T(r,t)}{\partial t} \qquad (1)$$

along with the boundary condition equation,

$$-\kappa \left.\frac{\partial T}{\partial r}\right|_{r=R} = G(T(r=R,t) - T_f), \qquad (2)$$

where κ and G are the thermal conductivity and thermal conductance, respectively, c_p is the isobaric heat capacity, R is the radius of gyration of the protein, $T(r, t)$ is the local temperature at position r and time t inside the protein, and T_f is the temperature of the surrounding fluid, which it is assumed to be constant. We note that the boundary condition given in eqn (2) is equivalent to a convective boundary condition.

Using the initial condition, $T(r, t = 0) = T_i$, the solution of eqn (2) is[39]

$$\frac{T(r,t)-T_f}{T_i-T_f} = 4\sum_{n=1}^{\infty}\frac{\sin(\lambda_n)-\lambda_n\cos(\lambda_n)}{2\lambda_n-\sin(2\lambda_n)}\exp\left(-\frac{\lambda_n^2 t}{\tau}\right)\frac{R}{\lambda_n r}\sin\left(\frac{\lambda_n r}{R}\right), \quad (3)$$

where $\tau = R^2/D_T$, D_T is the thermal diffusivity, $D_T = \kappa/(\rho c_p)$ The coefficients, λ_n, fulfil the following relation,

$$1-\lambda_n\cot(\lambda_n) = \frac{GR}{\kappa} = \mathrm{Bi}, \quad (4)$$

where Bi is the Biot number. The Biot number measures the ratio of the thermal resistance of the protein to the thermal resistance of the interface. A first order process normally corresponds to $\mathrm{Bi} \ll 1$. Considering a thermal conductance of $G \approx 10^2$ MW K^{-1} m^{-2}, typical of hydrocarbon–water interfaces,[30,37] a protein radius of gyration of $\approx$2 nm and a protein thermal conductivity of the order of 0.2 W K^{-1} m^{-1},[23] we get $\mathrm{Bi} \approx 1$. As we will see below, the thermal conductance of the protein–water interface is similar to that of the alkane–water interface. Hence, our estimate of $\mathrm{Bi} \approx 1$ indicates that the thermal resistance of the protein and the protein–water interface are of the same order, and both the thermal conductivity and the thermal conductance should be included in the diffusion equation to model the temperature relaxation process.

The solution of eqn (3) can be simplified by taking the average temperature over the whole volume, V, of the protein. This results in

$$\frac{\langle T(r,t)\rangle_V - T_f}{T_i-T_f} = \frac{T(t)-T_i}{T_i-T_f} = 6\sum_{n=1}^{\infty}\frac{1}{\lambda_n^3}\frac{(\sin(\lambda_n)-\lambda_n\cos(\lambda_n))^2}{\lambda_n-\sin(\lambda_n)\cos(\lambda_n)}\exp\left(\frac{-\lambda_n^2 t}{\tau}\right), \quad (5)$$

which can be further simplified by retaining only the first term in the series,[39] which represents a good approximation for $t > 0.2\,\tau$,

$$\frac{T(t)-T_f}{T_i-T_f} = 6\frac{1}{\lambda_1^3}\frac{(\sin(\lambda_1)-\lambda_1\cos(\lambda_1))^2}{\lambda_1-\sin(\lambda_1)\cos(\lambda_1)}\exp\left(\frac{-\lambda_1^2 t}{\tau}\right), \quad (6)$$

with

$$1-\lambda_1\cot(\lambda_1) = \frac{GR}{\kappa} = \mathrm{Bi}. \quad (7)$$

Eqn (6) is more convenient for the analysis of the simulation results and is the one we have employed in this work. From the fitting of the simulation results to eqn (6) we can obtain both the λ_1 parameter appearing in eqn (7) and τ. The fitting is performed as follows. We rewrite eqn (6) as:

$$\ln\frac{T(t)-T_f}{T_i-T_f} = A - t/B \quad (8)$$

where A includes the sin and cos terms and $B = \tau/\lambda_1^2$. The fitting of the temperature relaxation data to eqn (8) provides estimates for A and B. λ_1 is obtained from A and τ from B. The thermal conductivity follows from

$$\kappa = \frac{\rho c_p R^2}{\tau} = \frac{3C_p}{4\pi R\tau} \quad (9)$$

where R is the radius of gyration of the protein, ρ is the protein density, which we define as $\rho = m/V$, where m is the protein mass and $V = 4\pi R^3/3$, $C_p = mc_p$ (in J K^{-1}). Eqn (9) follows from $D_T = R^2/\tau = \kappa/(\rho c_p)$. Once κ is known, the thermal conductance (G) can be estimated using eqn (7). In addition to the analysis of the temperature relaxation, the computation of the thermal conductivity requires the heat capacity, C_p, and the radius of gyration of the proteins (*cf.* eqn (9)). The computation of the heat capacity is discussed below.

Using the approach outlined above we have estimated the thermal conductance of small alkane nanodroplets in water.[30] Our results for this quantity when extrapolated to a droplet of infinite radius were consistent with the estimates obtained for planar alkane–water interfaces using the stationary NEMD approach.[37] This lends support to the consistency of our method.

We note that the equations discussed above (3–6) are used to model heat relaxation in macroscopic objects too. We find that the relaxation in small objects such as proteins can be described in the same way as in larger macroscopic objects. One requirement for this to be true is that the velocity components of the atoms must follow a normal distribution, so that we can define a proper microscopic temperature. Deviations from normality if present are expected to appear more clearly in very small objects. Hence, to test this point we have chosen the smallest protein investigated in this work, myoglobin. Fig. 1 shows the normalized probability velocity distribution as well as the quantile–quantile (Q–Q) plot where we compare the velocity distribution generated in the simulation with a theoretical normal distribution. For this analysis we considered the velocities of the protein carbon atoms. The linearity of the Q–Q plot indicates that our simulation data are normally distributed. Application of the Shapiro–Wilk method (using 4000 samples)[40,41] did not show evidence of deviations from normality.

Computer simulations of the proteins

We have investigated three protein structures, myoglobin (1MBS entry in the Protein Data Bank),[42] green fluorescence protein (1QXT),[43] and two different states of the Ca^{2+}-ATPase (1SU4[4] and 1KJU[44]). The Ca^{2+}-ATPase enzymes are P-type ion pumps that feature in active transport of Ca^{2+} across the cellular membrane. The catalytic cycle involves several conformations. 1SU4 is a conformation where Ca^{2+} is present (E1 state), whereas 1KJU is a conformation corresponding to the Ca^{2+}-free (E2) state. It has been recently found that ATPases release heat when they are transporting Ca^{2+},[8] hence knowledge of the thermal transport properties is needed to characterize the heat transfer in these enzymes.

Snapshots of the proteins are given in Fig. 2. It can be seen that Ca^{2+}-ATPases undergo dramatic conformational changes during the enzymatic cycle.

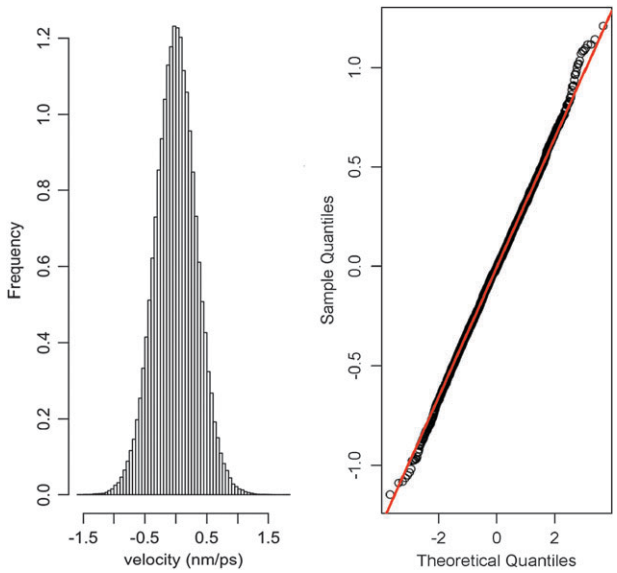

Fig. 1 (Left) Normalized probability distribution of velocities for myoglobin. (Right) Quantile–quantile plot to test the normality of the velocity distribution function; simulations (y-axis), normal distribution (x-axis).

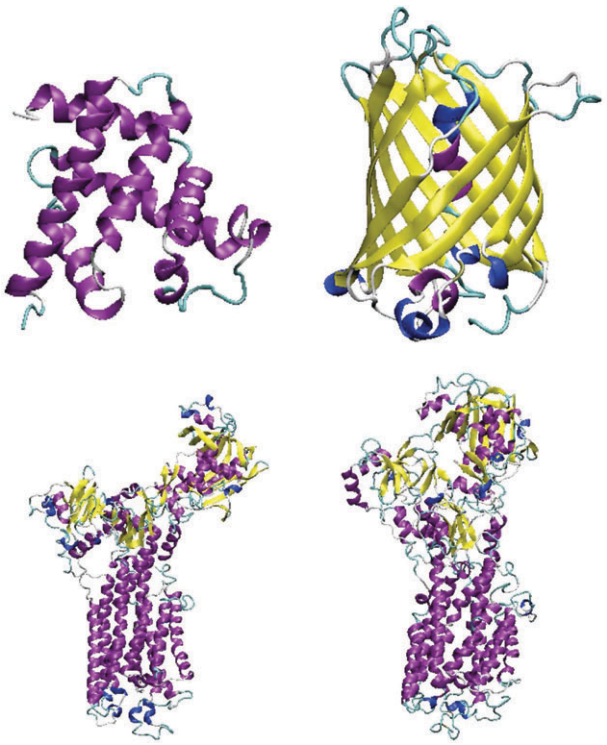

Fig. 2 Snapshots of the proteins investigated in this work. Myoglobin (top-left), GFP (top-right), 1SU4 (bottom-left) and 1KJU (bottom-right).

The protein interactions were modeled using the GROMOS96 43a2 force field.[45] The structure of the proteins was firstly minimized *in vacuo* using the steepest descent method. In order to perform the transient non-equilibrium simulations, the proteins were subsequently immersed in the center of a spherical water droplet with a diameter 9–10 nm (see Fig. 3). This droplet was large enough to solvate the different proteins without affecting their conformation. Water was modeled using the simple point charge-extended model (SPC/E).[46] All bonds in the proteins and water were kept rigid using the LINCS algorithm.[47] The van der Waals interactions were cut off at 1.7 nm. The Coulombic interactions were truncated at 1.5 nm using a switching function at 1.3 nm. The non-equilibrium simulations of the protein–water system were performed without periodic boundary conditions, and both the linear and angular momenta were removed.[48] To avoid the drift of the protein towards the droplet interface, we reset the center of mass motion of the protein and solvent separately. We note that the rotational motion of the protein and solvent are not coupled in the simulation timescale investigated in this work. Considering the protein as a sphere moving in a newtonian fluid we can estimate the relaxation time associated to the rotation, $\tau = 4\pi\eta R^3/(k_B T)$. Using the viscosity of water, $\approx 10^{-3}$ Pa s, the protein radius of gyration, ≈ 1 nm and $T = 300$ K results in relaxation times of the order of 25 ns. This is of the same order of magnitude as experimental estimates, 45 ns for myoglobin,[49] and much larger than the simulation times, 0.1 ns, employed to investigate the temperature relaxation process. Depending on the protein size the simulations involved 10^4 (for 1MBS and 1QXT) to 10^5 (for 1SU4 and 1KJU) solvent molecules, and a time step of 2 fs. Due to the low vapor pressure of water at 300 K, we did not observe any significant water evaporation during the simulations. Using this set up the root mean square deviation of the proteins in the water sphere with respect to the crystallographic structures was found to be of the order of 0.3 nm.

The transient non-equilibrium simulations were performed as follows. Firstly we equilibrated the whole system at constant temperature, 300 K. After this initial equilibration two Berendsen thermostats[50] were applied, one to the protein and the second one to the water droplet. These thermostats were applied for about 10 ps to allow the temperatures of the proteins and water to fluctuate around the corresponding target values T_i and T_f, respectively. After the equilibration period, the thermostat on the protein was removed and the

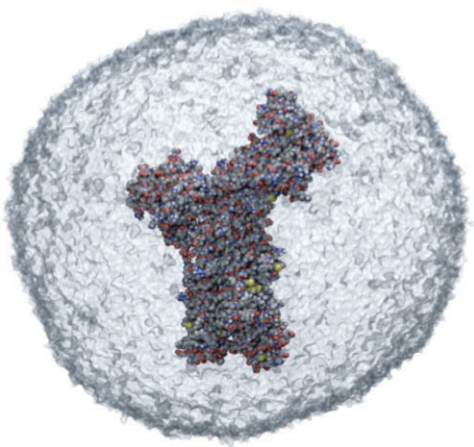

Fig. 3 Simulation set up employed in the transient non-equilibrium simulations, showing the protein Ca^{2+}-ATPase immersed in the water droplet.

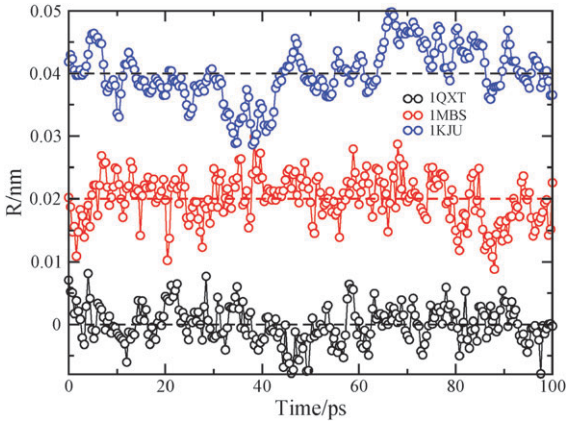

Fig. 4 Variation of the radius of gyration with time for three proteins investigated in this work. The simulation results correspond to a transient non-equilibrium simulation, where the initial temperature was set to 350 K. The radius of gyration for two of the proteins has been shifted upwards to facilitate the comparison of the results.

system was allowed to relax. The temperature of the water bath was maintained constant during the relaxation process using a temperature coupling constant of 0.1 ps. We performed several tests to assess the effect of the temperature coupling constant on the protein relaxation process. We found that the results were insensitive within statistical uncertainty to the value set for the coupling constant. We performed an additional test using a Nosé-Hoover (NH) thermostat to assess the influence of the thermostat. We found that both the Berendsen and NH reproduced the same relaxation behavior for the temperature. The relaxation process was investigated for about 100 ps. The equipartition principle expression was employed to compute the temperature of the protein as a function of time. The temperature was then fitted to eqn (6) using the Levenberg–Marquadt algorithm.[51] The results reported below were obtained from an analysis performed over three independent runs.

The computation of the thermal conductance requires previous knowledge of the effective radius of the proteins (radius of gyration) and the heat capacity (see eqn (9)). We found that the radius of gyration of the protein fluctuates around a well defined average during the 100 ps duration of the relaxation process (see Fig. 4).

The heat capacity of the proteins was estimated using constant temperature runs of the protein immersed in water using in this case periodic boundary conditions. The heat capacity was calculated from direct numerical differentiation of the internal energy of the protein using temperatures around the temperature of interest, $T = 300$ K. Typically we used 5 temperatures, 310, 305, 300, 295 and 290 K, to calculate the derivative of the internal energy. Each simulation was 1.2 ns long. All simulations were performed using the GROMACS simulation package.[52]

Results

Heat capacity of proteins

The heat capacity plays an important role in determining the energetics associated to protein folding processes. This property has been analyzed by Gomez *et al.*[53] using a wide range of proteins in different conformations. In that work it was established that the heat capacity of globular proteins in solution is dominated, about 80% of the total, by intramolecular contributions, including stretching, bending and internal rotations, with intermolecular degrees of freedom contributing only ≈3%. For proteins in solution it was concluded that there is a hydration contribution to the heat capacity which amounts to about 15% of the heat capacity of the proteins in their native states. Table 1 compares our results with experimental data available in the literature, which were obtained using calorimetric techniques. We have also included simulation data from Yu and Leitner,[23] who used a computational approach to estimate the heat capacities of myoglobin and GFP. Our results for the heat capacity of myoglobin are in good agreement with the experimental results of this protein in solution. The estimates from Yu and Leitner are slightly below the experimental result. We note that these simulations were performed in anhydrous conditions.

Table 1 Heat capacity of the proteins investigated in this work in kJ mol^{-1} K^{-1}. Simulations $T = 300$ K, experiments 298 K

Protein	This work	Experiments[54]	Simulations[23]
Myoglobin	27 ± 9	24.2	17
GFP	47 ± 10	—	24
Ca^{2+}ATP-ase (1SU4)	180 ± 35	—	—
Ca^{2+}ATP-ase (1KJU)	180 ± 30	—	—

Our results show a significant increase in the heat capacity in moving from myoglobin to GFP and to the Ca^{2+}-ATPases, both containing a larger number of carbon atoms, $\approx 10^3$ and $\approx 5 \times 10^3$, respectively, as compared with myoglobin $\approx 8 \times 10^2$. The heat capacity is an extensive property for macroscopic systems, but for small systems consisting of a few atoms the heat capacity is non extensive.[55] Hence our computations of the heat capacity of single proteins can provide a test to assess the extensivity of this property in proteins of varying molecular weight. A representation of the experimental heat capacity of the protein as a function of the number of carbon atoms offers an approach to test the consistency of the simulated heat capacities reported above (see Fig. 5). We note that more involved approaches are possible. Gomez *et al.*[53] considered the molecular weight and the accessible surface of the proteins, in order to fit heat capacities of proteins in the non-native state. Fig. 5 clearly shows that the experimental results follow a linear dependence with the number of carbon atoms, as would be expected from the extensive character of the heat capacity. Our simulation results conform to this linear behavior and in general are in good agreement with the experimental measurements. To the best of our knowledge there are no experimental results of the heat capacity of Ca^{2+}-ATPases. We find that the heat capacity of these proteins is of the order of 180 kJ mol^{-1} K^{-1}. This result agrees well with the heat capacity obtained from the extrapolation of the experimental results for smaller proteins (*cf.* Fig. 5). Within the statistical accuracy of our computations the heat capacities of the two Ca^{2+}ATPase conformations, 1SU4 and 1KJU, are the same, indicating the heat capacity is not sensitive to the structural detail of the proteins, and

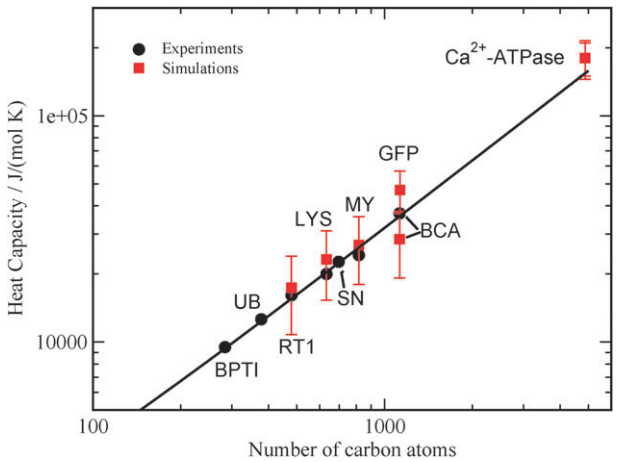

Fig. 5 Heat capacity of native proteins in solution as a function of the number of carbon atoms in the protein. Experiments 298 K, simulations 300 K. The experimental values (full circles) are taken from ref. 53. The labels denote different proteins; bovine pancreatic trypsin inhibitor (BPTI), ubiquitin (UB), rybonuclease T1 (RT1), lysozyme (LYS), staphylococcal nuclease (SN), myoglobin (MY), bovine chymotrypsinogen A (BCA), green fluorescence protein (GFP) and Ca^{2+}-ATP-ases. The squares represent the simulation results obtained in this work and the line is a linear fitting to the experimental data.

suggesting that the number of degrees of freedom for both conformations is very similar.

Thermal conductance and thermal conductivity of proteins

Fig. 6 shows a representative temperature relaxation curve for one of the proteins investigated in this work (Ca^{2+}-ATPase-1SU4). All the relaxation processes investigated here involved a time span of about 100 ps. We find that the time scale for temperature relaxation is tens of picoseconds. Assuming, as a first approximation, an exponential decay of the temperature with time, $\exp(-t/\tau)$ we can estimate a characteristic relaxation time, τ, for the cooling process. This is of the order of 10–20 ps for the proteins investigated in this work. We have fitted the simulated temperature relaxation data to eqn (6) to quantify the thermal diffusivity, thermal

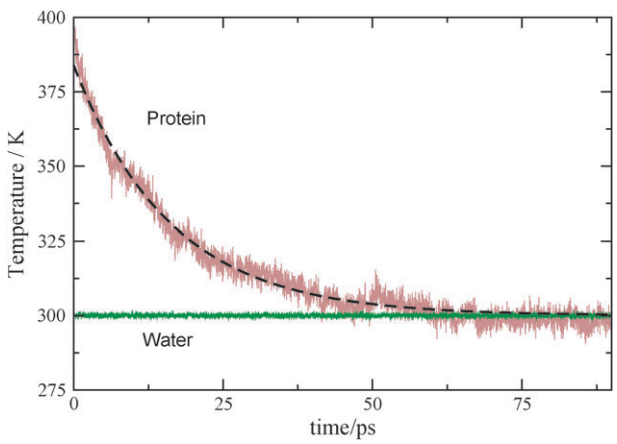

Fig. 6 Temperature relaxation of Ca^{2+}-ATPase (1SU4) as a function of time. The dashed line represents the fitting of the temperature relaxation to eqn (6).

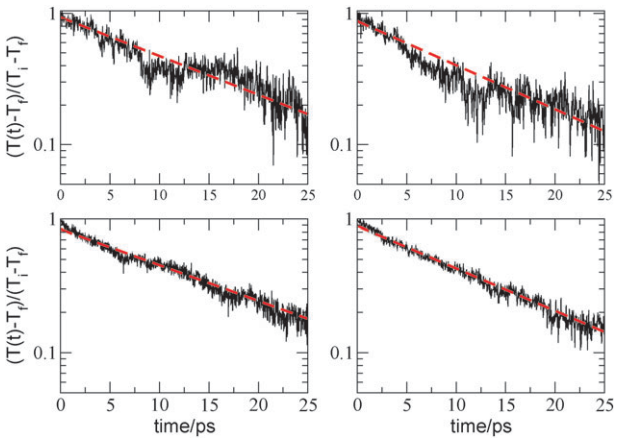

Fig. 7 Temperature relaxation of the four proteins investigated in this work: myoglobin (top-left), GFP (top-right), ATPase-1SU4 (bottom-left) and ATPase-1KJU (bottom-right). T_i and T_f represent the initial and solvent temperatures, 350 and 250 K, respectively. The dashed line represents the fitting of the temperature relaxation to eqn (6).

conductivity and the thermal conductance of the protein–water interface.

Fig. 7 shows the temperature relaxation results along with the corresponding fitting using eqn (6). Our model (eqn (6)), which takes into account the different thermal conductivities of the solvent and the protein, provides a good representation of the temperature relaxation. This is particularly clear for the larger proteins (ATPase) where the temperature fluctuations are significantly reduced as compared to the smaller proteins (*cf.* Fig. 7).

Table 2 contains numerical data of the heat transport properties of the proteins for (T_i, T_s) = (350, 250) K. To test the sensitivity of our results to the simulation conditions we performed simulations with different initial and solvent temperatures, (400, 300) K and (350, 250) K. We obtained the same results within the statistical accuracy of our method. Hence we report in Table 2 the results for (350, 250) K.

The thermal diffusivities obtained in this work are of the order expected for biological tissue[56] and they are also in the range of the thermal diffusivities of small alkane droplets in water 5–12 $Å^2$ ps^{-1}. Our results for the smaller proteins, myoglobin and GFP, ≈ 5 $Å^2$ ps^{-1} are similar to the thermal diffusivity of *Rhodospseudomonas viridis*, 7 $Å^2$ ps^{-1}, obtained by different authors[14] using a transient non-equilibrium approach similar to ours. Yu and Leitner[23] have employed more recently a different approach, based on the scaling of the

Table 2 Heat transport properties; thermal diffusivity (D) in $Å^2$ ps^{-1}, thermal conductivity (κ) in W K^{-1} m^{-1}, thermal conductance (G) in MW K^{-1} m^{-2}), radius of gyration (R) in nm, density (ρ) in kg m^{-3}, and the Kapitza length (l_K) in nm, of the proteins investigated in this work. All results correspond to temperature relaxations from T_i = 350 K to T_f = 250 K

Protein	D	κ	G	R	l_K
Myoglobin	4 ± 1	0.13 ± 0.02	100 ± 5	1.529 ± 0.003	1.3
GFP	3 ± 1	0.12 ± 0.01	270 ± 20	1.667 ± 0.002	0.4
ATPase-1SU4	17 ± 2	0.22 ± 0.02	260 ± 70	3.821 ± 0.004	0.9
ATPase-1KJU	16 ± 2	0.23 ± 0.03	210 ± 40	3.69 ± 0.01	1

energy diffusion coefficient with the vibrational mode frequency of the protein, to estimate the thermal diffusivity of myoglobin and GFP. These authors equilibrated the proteins in water before computing the transport properties *in vacuo*. Our results lie below the ones reported by these authors, 21.1 and 18.7 $Å^2$ ps^{-1} for GFP and myoglobin, respectively, although they are comparable in magnitude.

The thermal conductivities of the different proteins are comparable. We obtain values of the order of 0.15–0.2 W K^{-1} m^{-1}. These values are similar to the ones obtained in small hydrocarbon droplets,[30] and again they are comparable to the thermal conductivity reported by Yu and Leitner, 0.27 W K^{-1} m^{-1} using a different simulation approach. Our results show that all the proteins investigated in this work are worse heat conductors than water ($\kappa \approx 0.6$ W K^{-1} m^{-1}) and consequently they should develop larger temperature gradients as compared with bulk water.

The analysis of the temperature relaxation using the solution of the heat diffusion equation, (*cf.* eqn (6)) provides a route to estimate the thermal conductance of the protein–water interface. We note that the protein surface is heterogeneous in chemical composition, and irregular in shape, consisting of regions of different curvature. Because the complex surface topography of the proteins, consisting of curved and roughly planar areas, our results for the thermal conductance have to be interpreted as illustrative of the *average* or *effective* thermal conductance of the protein–water interface. Our thermal conductances of the protein–water interfaces 100–250 MW K^{-1} m^{-2}, are similar to the ones reported by us for hydrocarbon nanodroplets immersed in water, which are higher than the thermal conductances of planar alkane–water interfaces, 65 MW K^{-1} m^{-2}.[37] In particular, our estimate of the thermal conductance of GFP is in excellent agreement with recent results reported for this protein using a different simulation approach, (*i.e.* stationary non-equilibrium simulations), and a different protein force-field (*i.e.* full atom model).[28] These thermal conductances are of the order of the ones observed in water–hydrophilic interfaces,[57] indicating a strong thermal coupling between water and the protein surface. We have recently suggested that the thermal conductances of curved interfaces can be higher than those of planar interfaces.[30] This is a physical effect that goes beyond the chemical nature of the surface. Although it is not possible to disentangle surface topographic (curvature) and chemical (hydrophilic and hydrophobic patches) effects easily, we expect that similar curvature effects may apply to the protein–water interface, and hence, the corresponding thermal conductance may be higher than that of the corresponding planar interface.

Finally, using our simulation results we have estimated the Kaptiza length, which represents the thickness of a layer with thermal conductivity, κ, which has thermal conductance, G, *i.e.*, the same as the protein–water interface. The typical values for hydrophobic interfaces are of the order of 10 nm, as compared with 1 nm for hydrophilic interfaces.[57] We find Kapitza lengths of the order of $\approx$1 nm, *i.e.*, of the order of the radius of gyration of the proteins (see Table 2), showing that the interfacial conductance is important for defining the thermal transport of the biomolecules. This idea has been advanced in the discussion of the Biot number (*cf.* eqn (4)). The Biot number can be rewritten in terms of the Kapitza length as, $\mathrm{Bi} = R/l_K$. Hence, for $\mathrm{Bi} \approx 1 \Rightarrow l_K \approx R$, and both the thermal conductance and the thermal conductivity must be included in the description of the thermal relaxation.

Conclusions and final remarks

We have performed an investigation of the thermal properties of three structurally different proteins; myoglobin, GFP and Ca^{2+}-ATPase in water. Myoglobin and ATPases control different biological processes, oxygen transport, and active transport of Ca^{2+} across the cellular membrane, respectively. These proteins are dramatically different in structure and size, 17951 *vs.* 109706 Da. In order to obtain information on the transport properties of these biomolecules we have performed transient non-equilibrium molecular dynamics simulations, whereby we model the temperature relaxation of the protein towards the temperature of the surrounding bath. The analysis of the temperature relaxation with time offers an approach to extract the thermal conductivity and thermal diffusivity of the protein as well as the thermal conductance of the protein–water interface. With this purpose we have considered a solution of the diffusion equation that incorporates both the thermal conductivity of the protein and the thermal conductance as fitting parameters.

We find that the thermal conductivity of the proteins is low, 0.1–0.2 W K^{-1} m^{-1} as compared with the thermal conductivity of water, 0.6 W K^{-1} m^{-1}, hence proteins should be able to sustain large thermal gradients across their structure. This may have implications on biological processes involving molecular motors such as Ca^{2+}-ATPase. Following our estimates of the thermal conductivity, it seems feasible that these proteins are capable of maintaining temperature gradients under stationary conditions. According to the non-equilibrium thermodynamics theory[31–33] the development of such temperature gradient could then, due to reciprocity of phenomena, trigger uptake of Ca^{2+} as well as ATP-hydrolysis, pointing to a possible role of the Ca^{2+}-ATPase as a temperature regulator, as proposed by de Meis and coworkers.[58]

Within the statistical uncertainty of our computations we do not find significant differences in the thermal conductivities of the three proteins investigated in this work. The thermal diffusivity seems to be more sensitive to the protein nature though, with an increase in this property of about three times in going from the smaller proteins (myoglobin and GFP) to the larger ones (Ca^{2+}-ATPase). The thermal conductances of the three proteins vary from 100 to 270 MW K^{-1} m^{-2}, myoglobin showing the lower thermal conductance of all the systems investigated. Our results for the heat capacity show good agreement with available experimental data of proteins obtained from calorimetric measurements. In addition to the proteins listed above we performed simulations of the heat capacity of lysozyme, rybonuclease T1, and bovine chymotrypsinogen (BCA). All are in good agreement with the experiment, with BCA showing the largest deviations from the experimental data. The heat capacity correlates linearly with the number of carbon atoms of the proteins, as expected for an extensive property. Using this result and the experimental data of

small proteins, we have estimated the heat capacity of the Ca^{2+}-ATPase. The extrapolated result is in excellent agreement with our computational estimate of 180 kJ mol^{-1} K^{-1}. To the best of our knowledge this is the first computational estimate of the heat capacity of this important protein.

Our work, in conjunction with previous investigations, offers a consistent image of the heat transport in biomolecules. The thermal conductance of the water–protein interface should play a relevant role in controlling the energy relaxation of the protein. Overall, our results show that the water–protein interface has a high conductance, similar to the one measured in water adsorbed at hydrophilic surfaces.[57] We suggest that in addition to the heterogeneous chemical structure of the proteins, with hydrophobic and hydrophilic patches, other factors such as the surface topography, characterized by highly curved interfaces, may be contributing to the enhancement of the thermal conductance of these nanoscale interfaces. We believe this information is relevant to construct microscopic models to describe how the energy is redistributed in proteins and through the water–protein interface. In the long term, these fundamental studies may be useful to understand from a microscopic perspective certain human diseases, *e.g.*, muscular dystrophy and sickle cell disease, as well as temperature regulation in muscle tissue, which have been linked to the Ca^{2+}-ATPase protein.[58,59]

Acknowledgements

We would like to thank the Imperial College High Performance Computing Service and NOTUR (The Norwegian metacentre for computational science), for providing computational resources. Funding from the Center for Advanced Study, at the Norwegian Academy of Sciences and Letters is gratefully acknowledged.

References

1 P. K. Agarwal, *J. Am. Chem. Soc.*, 2005, **127**, 15248–15256.
2 J. F. Swain and L. M. Gierasch, *Curr. Opin. Struct. Biol.*, 2006, **16**, 102–108.
3 J. Ross, *J. Phys. Chem. B*, 2006, **110**, 6987–6990.
4 C. Toyoshima, M. Nakasako, H. Nomura and H. Ogawa, *Nature*, 2000, **405**, 647–655.
5 S. W. Lockless and R. Ranganathan, *Science*, 1999, **286**, 295–299.
6 E. R. Henry, W. A. Eaton and R. M. Hochstrasser, *Proc. Natl. Acad. Sci. U. S. A.*, 1986, **83**, 8982–8986.
7 V. Botan, E. H. G. Backus, R. Pfister, A. Moretto, M. Crisma, C. Toniolo, P. H. Nguyen, G. Stock and P. Hamm, *Proc. Natl. Acad. Sci. U. S. A.*, 2007, **104**, 12749–12754.
8 M. Suzuki, V. Tseeb, K. Oyama and S. Ishiwata, *Biophysical Journal: Biophysical Letters*, 2007, **92**, L46–L48.
9 F. Bresme, A. Lervik, D. Bedeaux and S. Kjelstrup, *Phys. Rev. Lett.*, 2008, **101**, 020602.
10 D. M. Leitner, *Annu. Rev. Phys. Chem.*, 2008, **59**, 233–259.
11 Y. Mizutani and T. Kitagawa, *Science*, 1997, **278**, 443–446.
12 R. H. Austin, A. Xie, L. van der Meer, B. Redlich, P. A. Lindgoard, H. Frauenfelder and D. Fu, *Phys. Rev. Lett.*, 2005, **94**, 128101.
13 R. J. D. Miller, *Annu. Rev. Phys. Chem.*, 1991, **42**, 581–614.
14 M. Tesch and K. Schulten, *Chem. Phys. Lett.*, 1990, **169**, 97–102.
15 P. Li and P. M. Champion, *Biophys. J.*, 1994, **66**, 430–436.
16 K. Blumhagen, I. Muegge and E. W. Knapp, *Int. J. Quantum Chem.*, 1996, **59**, 271–279.
17 K. Moritsugu, O. Miyashita and A. Kidera, *Phys. Rev. Lett.*, 2000, **85**, 3970–3973.
18 D. M. Leitner, *Phys. Rev. Lett.*, 2001, **87**, 188102.
19 D. E. Sagnella, J. E. Straub and D. Thirumalai, *J. Chem. Phys.*, 2000, **113**, 7702–7711.
20 D. E. Sagnella and J. E. Straub, *J. Phys. Chem. B*, 2001, **105**, 7057–7063.
21 K. Moritsugu, O. Miyashita and A. Kidera, *J. Phys. Chem. B*, 2003, **107**, 3309–3317.
22 X. Yu and D. M. Leitner, *J. Phys. Chem. B*, 2003, **107**, 1698–1707.
23 X. Yu and D. M. Leitner, *J. Chem. Phys.*, 2005, **122**, 054902.
24 N. Ota and D. A. Agard, *J. Mol. Biol.*, 2005, **351**, 345–354.
25 T. Ishikura and T. Yamato, *Chem. Phys. Lett.*, 2006, **432**, 533–537.
26 K. Sharp and J. J. Skinner, *Proteins: Struct., Funct., Bioinf.*, 2006, **65**, 347–361.
27 M. Takayanagi, H. Okumura and M. Nagaoka, *J. Phys. Chem. B*, 2007, **111**, 864–869.
28 N. Shenogina, P. Keblinski and S. Garde, *J. Chem. Phys.*, 2008, **129**, 155105.
29 M. J. Assael, E. Charitidou, C. A. N. de Castro and W. A. Wakeham, *Int. J. Thermophys.*, 1987, **8**, 663–670.
30 A. Lervik, F. Bresme and S. Kjelstrup, *Soft Matter*, 2009, **5**, 2407–2414.
31 S. Kjelstrup, J. M. Rubi and D. Bedeaux, *Phys. Chem. Chem. Phys.*, 2005, **7**, 4009–4018.
32 D. Bedeaux and S. Kjelstrup, *Phys. Chem. Chem. Phys.*, 2008, **10**, 7304–7317.
33 S. Kjelstrup, D. Barragan and D. Bedeaux, *Biophys. J.*, 2009, **96**, 4376–4386.
34 T. Ikeshoji and B. Hafskjold, *Mol. Phys.*, 1994, **81**, 251–261.
35 F. Bresme, B. Hafskjold and I. Wold, *J. Phys. Chem.*, 1996, **100**, 1879–1888.
36 F. Bresme, *J. Chem. Phys.*, 2001, **115**, 7564–7574.
37 H. A. Patel, S. Garde and P. Keblinski, *Nano Lett.*, 2005, **5**, 2225–2231.
38 S. Kjelstrup and D. Bedeaux, *Non-equilibrium Thermodynamics of Heterogeneous Systems 2008*, Series on Statistical Mechanics, World Scientific, Singapore, Singapore, vol. 16, 2008.
39 F. P. Incropera, D. P. DeWitt, T. L. Bergman and A. S. Lavine, *Fundamentals of Heat and Mass Transfer*, John Wiley & Sons, Hoboken, USA, 6th edn, 2006.
40 S. Shapiro and M. Wilk, *Biometrika*, 1965, **52**, 591–611.
41 P. Royston, *Statistical Algorithms*, 1995, **44**, 547–551.
42 H. Scouloudi and E. Baker, *J. Mol. Biol.*, 1978, **126**, 637–660.
43 D. Barondeau, C. Putnam, C. Kassmann, J. Tainer and E. Getzoff, *Proc. Natl. Acad. Sci. U. S. A.*, 2003, **100**, 12111–12116.
44 C. Xu, W. J. Rice, W. He and D. L. Stokes, *J. Mol. Biol.*, 2002, **316**, 201–211.
45 L. D. Schuler, X. Daura and W. F. van Gunsteren, *J. Comput. Chem.*, 2001, **22**, 1205–1218.
46 H. J. C. Berendsen, J. R. Grigera and T. P. Straatsma, *J. Phys. Chem.*, 1987, **91**, 6269–6271.
47 B. Hess, H. Bekker, H. Berendsen and J. Fraaije, *J. Comput. Chem.*, 1997, **18**, 1463–1472.
48 S. C. Harvey, R. K.-Z. Tan and T. E. Cheatham-III, *J. Comput. Chem.*, 1998, **19**, 726–740.
49 G. South and E. Grant, *Proc. R. Soc. London, Ser. A*, 1972, **328**, 371–387.
50 H. J. C. Berendsen, J. P. M. Postma, W. F. van Gunsteren, A. DiNola and J. R. Haak, *J. Chem. Phys.*, 1984, **81**, 3684–3690.
51 W. H. Press, S. A. Teukolsky, W. T. Vetterling and B. P. Flannery, *The Art of Scientic Computing*, 3rd ed., Cambridge University Press, Cambridge, UK, 2007.
52 D. van der Spoel, E. Lindahl, B. Hess, G. Groenhof, A. Mark and H. Berendsen, *J. Comput. Chem.*, 2005, **26**, 1701–1718.
53 J. Gomez, V. J. Hilser, D. Xie and E. Freire, *Proteins: Struct., Funct., Genet.*, 1995, **22**, 404–412.
54 P. Privalov and G. Makhatadze, *J. Mol. Biol.*, 1990, **213**, 385–391.
55 T. L. Hill, *Thermodynamics of small systems*, Dover, Mineola, New York, 2002.
56 Y. Touloukian, R. Powell, C. Ho and M. Nicolaou, *Thermophysical Properties of Matter*, Plenum Press, New York, 1973.
57 Z. Ge, D. G. Cahill and P. V. Braun, *Phys. Rev. Lett.*, 2006, **96**, 186101.
58 L. de Meis, G. Oliveira, A. Arruda, R. Santos, R. da Costa and M. Benchimol, *Life*, 2005, **57**, 337–345.
59 E. Carafoli, *Physiological Reviews*, 1991, **71**, 129–153.